AIP | Review of Scientific Instruments

Time-of-flight mass spectrometry of mineral volatilization: Toward direct composition analysis of shocked mineral vapor

Daniel E. Austin, Andy H. T. Shen, J. L. Beauchamp, and Thomas J. Ahrens

Citation: Rev. Sci. Instrum. **83**, 044502 (2012); doi: 10.1063/1.4705745
View online: http://dx.doi.org/10.1063/1.4705745
View Table of Contents: http://rsi.aip.org/resource/1/RSINAK/v83/i4
Published by the American Institute of Physics.

Time-of-flight mass spectrometry of mineral volatilization: Toward direct composition analysis of shocked mineral vapor

Daniel E. Austin,[1,a)] Andy H. T. Shen,[2,b)] J. L. Beauchamp,[1] and Thomas J. Ahrens[2,c)]
[1]*Division of Chemistry and Chemical Engineering, California Institute of Technology, Pasadena, California 91125, USA*
[2]*Division of Geological and Planetary Sciences, California Institute of Technology, Pasadena, California 91125, USA*

(Received 2 November 2011; accepted 8 April 2012; published online 25 April 2012)

We have developed an orthogonal-acceleration time-of-flight mass spectrometer to study the volatiles produced when a mineral's shock-compressed state is isentropically released, as occurs when a shock wave, driven into the mineral by an impact, reflects upon reaching a free surface. The instrument is designed to use a gun or explosive-launched projectile as the source of the shock wave, impact onto a flange separating a poor vacuum and the high vacuum (10^{-7} Torr) interior of the mass spectrometer, and transmission of the shock wave through the flange to a mineral sample mounted on the high-vacuum side of the flange. The device extracts and analyzes the neutrals and ions produced from the shocked mineral prior to the possible occurrence of collateral instrument damage from the shock-inducing impact. The instrument has been tested using laser ablation of various mineral surfaces, and the resulting spectra are presented. Mass spectra are compared with theoretical distributions of molecular species, and with expected distributions from laser desorption. © *2012 American Institute of Physics*. [http://dx.doi.org/10.1063/1.4705745]

INTRODUCTION

Impact events are a dominant process in planetary formation and evolution. During an impact event, kinetic energy of the impactor drives both physical and chemical changes in the immediate event vicinity. Depending on the impact velocity and on constitutive and thermodynamic properties of both impactor and target, impacted media are partially or completely converted to liquid, gas, or even an ionized state.[1,2] In addition, chemical reactions, including dissociation and recombination, can take place within the resultant fluid phases, especially in gas-phase and ionized species.[3–5] Understanding the chemical changes associated with impacts is essential to understanding the impact accretion planetary formation process as it occurs on different lengths and timescales upon the initial differentiation and evolution of planets. Toward the end of the Earth's accretion, impacts from the increasingly larger planetesimals (which themselves accreted to masses within the planetary range) resulted in at least one giant collision that is hypothesized to have resulted in Moon formation.[6–8] It appears likely that giant impacts led to further processing of the Earth and other planetary surfaces. On Earth-like planets, after the creation of the initial atmosphere, and later, the biosphere, large impacts are thought to have induced substantial transients in global climate, and for only giant events, these transients appear to have affected the evolution of life on Earth. Similarly, understanding the chemistry of smaller impacts—especially micrometeorites—is necessary for interpretation of data from planetary missions such as Stardust,[3] as well as for studies of impact-induced formation of organic species.[9,10]

The mass extinction at the Cretaceous-Tertiary (K-T) boundary, 65 million years ago, is believed to be the result of global environmental changes caused by an impacting asteroid,[11] but the nature of specific changes that took place remains uncertain. Several models have been proposed, differing partially by varying assumptions about the chemical speciation of materials vaporized or aerosolized during the impact. Large quantities of released CO_2 (from calcite) or H_2O could have produced a greenhouse effect.[12] Alternatively, SO_2 or SO_3 released from gypsum and anhydrite present at the impact site may have been converted to sulfurous or sulfuric acids, creating acid rain or aerosol clouds.[13–15] Carbon monoxide has also been proposed as the dominant product, significantly modifying global atmospheric chemistry.[16] Other proposed mechanisms include global cooling from a blanket of dust or soot,[17] acid rain from nitric acid,[18,19] and radiative heating.[20] Identifying the most likely of these proposed mechanisms requires knowing the amounts of each chemical species released during the impact.

Hypotheses about chemical speciation in such an event are challenging to test either theoretically or experimentally. Scaling the results of small-scale experiments to a large-scale event requires numerous assumptions, such as the extent to which species reach chemical equilibrium in the impact plume, and the kinetics of all reactions. Regardless of the extent to which a plume approaches chemical equilibrium, predicting the final chemical species requires knowing the original species vaporized by the shock/rarefaction wave.

In three previous experiments designed to study impact chemistry, Boslough,[21] Tingle,[22] and Tyburczy[23] used a gun to launch metal projectiles onto mineral samples. The vapor

[a)]Author to whom correspondence should be addressed. Electronic mail: austin@chem.byu.edu. Present address: Department of Chemistry and Biochemistry, Brigham Young University, Provo, Utah 84602, USA.
[b)]Present address: Gemological Institute of America, 5355 Armada Drive, Carlsbad, California 92008, USA.
[c)]Deceased.

produced in the impacts was collected and later analyzed by mass spectrometry, however, post-impact reactions (i.e., on the vessel wall) and contamination from the projectile propellant may have affected or obscured some of the chemistry of the system. Studies using electrostatically accelerated microparticles have also been carried out in which impact-generated ions were analyzed *in situ* using time-of-flight mass spectrometry.[5,24–31] These studies have been limited to metal, polymer, and coated particles, and have not studied minerals of interest to the question of chemical speciation in impacts. Kawaragi used mass spectrometry and isotopic labeling to identify the gaseous species produced in pressed calcium carbonate powder samples shocked using a laser-accelerated flyer plate.[16] In any case, *in situ* composition measurements of the vapor produced in impacts of mineral samples remain to be made.

We are developing an instrument that would allow direct, *in situ* mass spectrometric measurements of the vapor produced at the free surface of a mineral subject to a shock wave. This instrument, the impact vaporization mass spectrometer (IVMS), is designed to be used in conjunction with a light-gas gun or explosive shock source, but a preliminary demonstration of the instrument capabilities utilized a pulsed nitrogen laser to produce mineral vapor. Rapid ionization, extraction, and analysis of vaporized neutrals allow the instrument to be used in a setting in which the mineral sample is destroyed (and possibly, after data are reported, mass spectrometer vacuum is broken on account of late-time collateral impact-induced damage). Because species released from the mineral sample are extracted and analyzed immediately upon formation, and because of the speed of time-of-flight mass spectrometry, the analysis can be completed prior to introduction of any contaminants from the projectile, propellant, or atmosphere. These sources of potential contamination can be effectively excluded from the analysis even if vacuum is broken.

This paper focuses on instrument design and operation. A preliminary demonstration of instrument performance, in which a pulsed laser is used to produce mineral vapor from calcite and gypsum, is also presented. Laser vaporization results are discussed both in the context of instrument performance and also in comparison to calculated equilibrium speciation for the minerals used.

METHODS

Figure 1 shows the design of the orthogonal acceleration time-of-flight mass spectrometer for analysis of impact-induced mineral vaporization. The device consists of the mounted mineral sample, the ionization region, collimation optics, a push-out pulser, drift tube, and ion detector. The instrument is housed in a custom-built vacuum chamber using standard con-flat flanges wherever possible. With the gate valve to the tubromolecular pump open, the vacuum pressure in the time-of-flight drift tube is 3×10^{-7} Torr (uncorrected), and is expected to be similar in all other areas of the vacuum chamber.

A thin, polished mineral sample is mounted onto a driver plate such that one surface of the mineral is in the high-vacuum region of the mass spectrometer, and the other surface is in physical contact with the driver plate. Samples used in preliminary demonstrations were 5–7 mm in diameter and 100 μm thick, double polished. The sample size and polish were chosen to provide a compromise between ease of manufacture and the amount of material that would be released into the system under high-velocity impacts. An accelerated projectile strikes the driver plate, and the resulting shock is transmitted to the mineral sample. As the shock wave reaches the free surface of the mineral, neutrals and some ions are produced. For calibration experiments the samples were simply epoxied to the driver plate, but for impact experiments the method of mounting and degree of physical contact will be important.

Directly in front of the mineral surface is an electrode grid (Ni electroformed mesh, 90% transmission, Buckbee Mears, St. Paul, MN), the potential of which can be varied to select either evolved ions or neutrals for further analysis. Past this plate is the electron ionization region, in which an electron beam is directed. The electron energy was chosen to be 70 eV at the point of impact with the neutrals so that ionization efficiencies and fragmentation patterns will be similar to the majority of previous work using electron ionization.[32] A small fraction of the neutral species (typically 1 in 10^4–10^6) is ionized as they pass through the electron beam. The electron current (typically <100 μA) is monitored by a custom-built Faraday cup detector, mounted on the opposite side of the ionization region. The electron beam is on continuously during an experiment. Immediately past the electron beam, and constituting the end of the ionization region, is an extraction grid. After ions pass through the extraction grid they are accelerated through 100 V to draw them quickly into the collimating ion optics. The residence time of neutrals/ions in the ionization region is on the order of 5–10 μsec based on typical molecular velocities and the dimensions of the ion optics, which is comparable to typical ion residence times in conventional electron ionization sources. A small electric potential (several volts) in the ionization region is used to extract newly formed ions more quickly than thermal velocities would otherwise carry them. This field also bends the electron beam through the ionization region, so two sets of compensating deflection plates (not shown in Figure 1) are used to steer the electron beam.

Mass resolution in orthogonal acceleration TOF is directly related to the degree of collimation of the ion beam at the point of the orthogonal push-out pulse. An Einzel lens is used to collimate the ion beam. The beam then enters the orthogonal acceleration region, where a push-out pulse sends a portion of the ions into the mass spectrometer drift tube. The timing of the push-out pulse is critical: the pulse must be timed to coincide with the bulk of the ion beam. Presumably, there will be some temporal distribution of neutrals produced from the shock wave, and there will also be a distribution of initial kinetic energies among these neutrals, so ions will reach the orthogonal acceleration region over a finite time period. Varying the timing of push-out pulse relative to the vaporization event may allow a rough time history to be compiled which would add further understanding to the vaporization process. It is expected that species created as ions at the

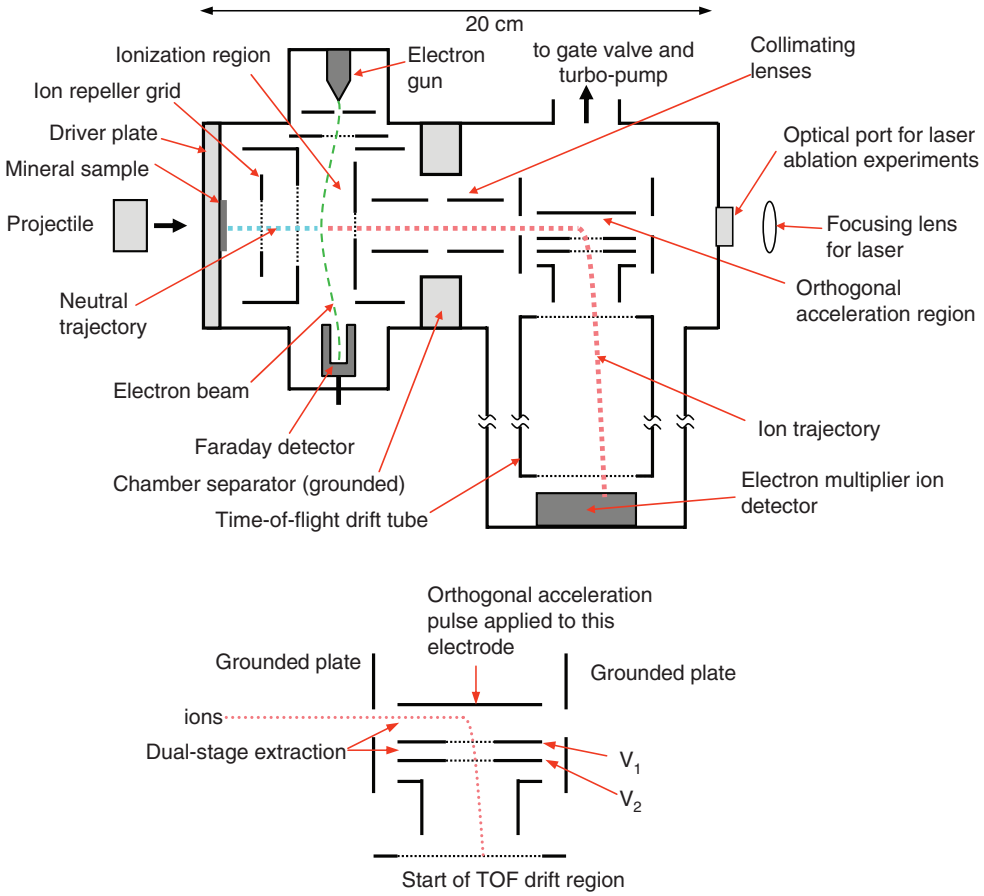

FIG. 1. Schematic of the impact vaporization mass spectrometer. Top: a high-velocity projectile strikes a driver plate, onto which is mounted a thin, polished mineral sample. The resulting shock wave releases neutral and ionic species from the mineral. In laser calibration experiments, ionization is realized by focusing a pulsed nitrogen laser onto the mineral. Neutrals released from the mineral are ionized by the electron beam, and the resulting ions are collimated, then pulsed into a time-of-flight mass spectrometer. Ions created at the mineral surface are similarly analyzed, but without the additional electron-ionization step. Ions can be excluded from analysis of neutrals using a repelling grid near the sample. Neutrals are not detected during analysis of ions be turning off the electron beam. Below: an enlargement of the orthogonal acceleration region showing representative ion trajectories. The use of two extraction grids at different voltages (dual-stage extraction) pushes the space-focus plane of ions out to the ion detector for improved mass resolution.

surface will, on average, reach the orthogonal acceleration region faster than species created as neutrals and ionized by the electron beam, so timing of the pulse must take into account also whether ions or neutrals are being analyzed.

The drift tube is electrically floated at −2000 V in order to keep other instrument components—especially the ionization and acceleration regions—at potentials near ground. Ions are accelerated using dual-stage extraction, pass through a 1.3 m drift tube, and are detected using an electron multiplier detector (ETP discrete dynode type, SGE Analytical, Austin, TX). The ion time-of-flight signal is amplified using a fast preamplifier (Ortec VT-120, Oak Ridge, TN), then digitized and recorded using a 200 MHz digital storage oscilloscope (Tektronix, Beaverton, OR). The original system design included a reflectron to improve resolution. However, for lighter molecular species, this level of resolution is not needed, so a straight drift tube was used instead.

The IVMS instrument is designed so that mineral samples can be shocked using a high-velocity projectile. For faster or larger projectiles, the driver plate will be damaged, and the vacuum system compromised during the experiment. In addition, the projectile will continue its forward motion after initial contact with the driver plate, and may destroy ion optics in the ionization and pulsed-acceleration regions. Although a thicker driver plate might alleviate this problem, it would likely result in attenuation of the shock wave and reduced vaporization at the mineral surface. The instrument design is such that ions are produced and promptly accelerated to a sufficiently high velocity that ions will reach the detector before inrushing gases and physical damage compromise the instrument. The ion optics and possibly the ion detector will be destroyed during each impact experiment and will need frequent replacement. The electronics and other components are isolated and set up in such a way as to minimize damage, and also to ensure that downstream components are not affected until after the ions are clear of that area of the instrument. The vacuum chamber can be isolated from the pumping system by a gate valve immediately prior to the experiment, so as to minimize pump damage if vacuum is compromised due to penetration of the impactor through the drive plate. Once this gate valve is closed, vacuum pressure will start to rise in the main chamber, so the experiment must be conducted promptly. For smaller projectiles this step is not necessary.

Initial testing of this instrument design was carried using a pulsed laser, rather than a projectile, to vaporize the surface of mounted mineral samples. A pulsed nitrogen laser, 337 nm,

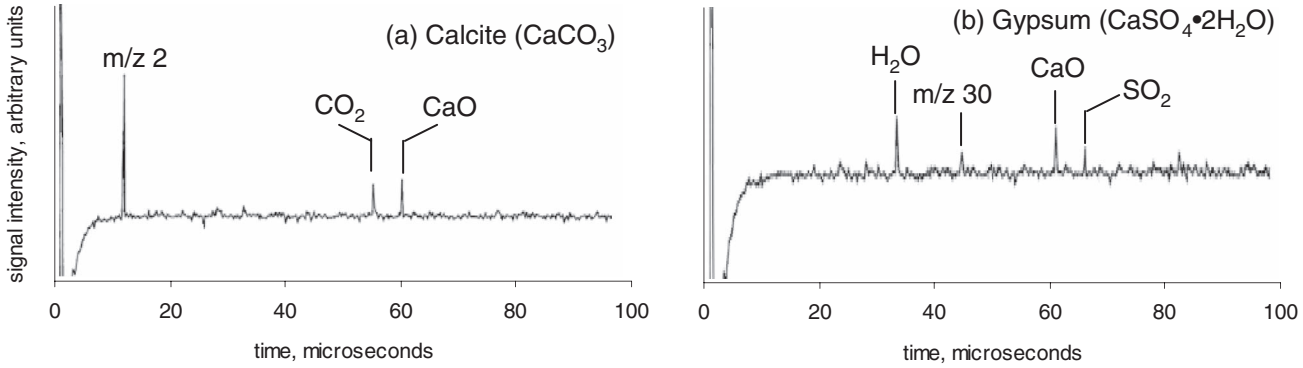

FIG. 2. Spectra of (left) calcite, and (right) gypsum samples using laser desorption and electron ionization. These spectra represent neutrals produced during the laser desorption that were subsequently ionized. Ions produced during the laser desorption were excluded from this analysis by the electrostatic deflection grid.

300 mJ/pulse, 4 μsec pulsewidth, was focused using standard optics to a small ($\ll$1 mm) spot size on the mineral samples. The laser was brought in through a viewport at the end of the vacuum chamber (see Figure 1). Although having the focusing optics so far from the sample (25 cm) is not optimal for laser ionization, it is adequate for instrument calibration. Under these conditions, both ions and neutrals were produced from the laser pulse. Analysis of the laser-generated ions was conducted by simply extracting the ions through the collimation region with the electron beam turned off. Analysis of neutrals was accomplished by repelling ions with the electrode plate in front of the mineral, and allowing only neutrals into the electron ionization region. The orthogonal push-out pulse was set to a 20 μsec delay after the laser firing, and had a rise time on the order of 300 ns and an amplitude of 600 V. Minerals used in these laser experiments included calcite ($CaCO_3$) and gypsum ($CaSO_4 \cdot 2H_2O$).

To supplement the experimental results, chemical equilibrium calculations on gypsum were carried out using the TOP20 thermodynamic modeling program. Speciation of both neutral and ionized species at various temperatures were calculated in order to compare with the results of the laser desorption experiments. The pressure in all calculations was held at 1×10^{-3} bar in order to approximate the ablated material in vacuum.

RESULTS AND DISCUSSION

Figure 2 shows time-of-flight mass spectra of laser-desorbed neutrals from calcite and gypsum samples in the IVMS instrument, using the laser setup and conditions described above. In the spectrum of neutrals produced from calcite, observed peaks include those for CO_2 and CaO, with an additional strong peak at m/z = 2. The peak at m/z = 2 could correspond to H_2, which is unexpected. A peak for H_2^+ (formed as an ion in the impact) has been observed in microparticle impact experiments, and has been suggested as being formed in a recombination reaction just above the sample surface.[5] Neutral H_2 may also be formed in such a case. The H_2 peak could also be due to adsorbed hydrogen on the calcite surface. Bulk calcite should be free from hydrogen.

The spectrum of neutrals evolved from gypsum shows peaks for electron-ionized H_2O, CaO, and SO_2, and an unidentified peak at m/z = 31. The presence of water is not unexpected from a hydrate mineral. Calcium oxide is present, as it was with calcite. The peak at 31 is small and could be due to noise, or could be caused by the fragment ion, S^+, with poor mass accuracy. Peaks for molecular or atomic hydrogen are absent. The peaks in these spectra show better than unit mass resolution.

Figure 3 shows the theoretical speciation at equilibrium of both neutrals and ions for gypsum, calculated using

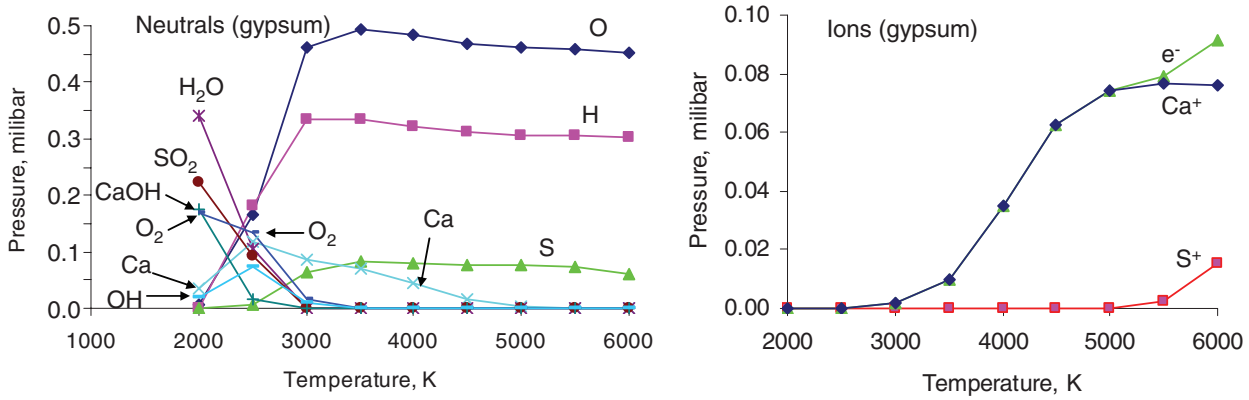

FIG. 3. Neutral (left) and ionic (right) species present at thermodynamic equilibrium for gypsum ($CaSO_4 \cdot 2H_2O$), 10^{-3} bar total pressure, as a function of temperature, calculated using TOP20. Molecular species dominate at lower temperatures, with ionic species increasing with higher temperatures. Partial pressures are normalized for a total pressure of 1 millibar at maximum temperature.

TOP20. Calculations of calcite show similar trends. At low temperatures, the molecular species H_2O, SO_2, CaOH, and O_2 dominate, while at higher temperatures only atomic neutrals are expected. Most of the speciation reactions occur in neutral species at relatively low temperatures (2000–3000 K). The experimental spectrum of gypsum shows only polyatomic species, implying a similarly low temperature. Of course, under laser desorption a system may not be at chemical equilibrium, but the general trends do provide some information about the energy range at which volatiles are produced. In addition, fragmentation may occur by different mechanisms between thermal equilibrium systems and rapidly heated systems produced by a pulsed laser. In the above spectra, no pairs of peaks corresponding to electron-impact fragmentation are visible; however, the low intensity of all peaks makes it difficult to make any conclusions about ion fragmentation.

For shock-induced vaporization as well as laser desorption, fragment ions could be created by one of two mechanisms: fragmentation as species are desorbed from the mineral surface, or fragmentation as a result of electron ionization. Understanding the former effect requires an estimate of the magnitude of the latter effect. In laser desorption, fragmentation is strongly dependent on laser power, and can range from no fragmentation to complete atomization, similar to the effect of temperature in Figure 3. As a result, no information about this process can be obtained from the experiments reported in this paper. Electron ionization of most molecules produces fragmentation, although some molecules will be ionized and detected intact. The extent of electron-induced fragmentation will vary between different molecular species, as also the electron ionization efficiency will vary, but both can be taken into account through calibration using pure compounds. For sulfate minerals, the speciation between SO_3 and SO_2 at the surface is of particular interest, so the degree of fragmentation of SO_3 from electron ionization will need to be determined and taken into account in future work.

The relationship between laser-induced ions and neutrals, and those produced by an impact has been detailed by Kissel and Kreuger.[2] Laser irradiation provides primarily electronic excitation, while an impact deposits energy primarily through lattice distortion. Both methods produce ions and neutrals, however, laser irradiance produces roughly 100 times more ionization than an impact at a given energy density.[2] Both methods produce vapor with similar efficiency. For the present study, the energy density delivered by the laser was not directly measured (which would require an accurate measure of the focused spot size). Because the total energy per pulse of 300 mJ produced a measurable quantity of neutral species, shock-induced vaporization with energy down to at least this level is expected to work in this system.

The time history of vaporization is convoluted with the distribution in initial kinetic energies of neutrals and ions. However, to a limited extent both of these effects can be explored with this experimental setup. Varying the orthogonal push-out pulse will sample ions that have reached the push-out region at different times. This time variation is the result of both the spread in time of formation of evolved neutrals and the initial kinetic energy. Faster neutrals evolved later may reach the push-out pulse region at the same time as slower, earlier neutrals. Assuming a spread of 100 m/s in initial velocities, resolution of the time at which neutrals are evolved is limited to 20 μsec. Conversely, if the neutral evolution is much shorter than this, the measured time history will be dominated by the initial velocity spread, which can then be measured. Observing the time history of evolved ions—species formed as ions on the surface—will indicate the timescale of evolved neutrals.

CONCLUSIONS

An orthogonal-extraction time-of-flight mass spectrometer has been developed for characterization of shocked-induced mineral vaporization. Initial experiments using laser ablation/ionization of mineral surfaces demonstrate the performance of the ion optics and electron ionization. Future experiments using this system are planned using small explosive-driven projectiles, which will allow fine-tuning of the experimental procedure before destructive experiments with larger projectiles.

ACKNOWLEDGMENTS

Contribution No. 8891 of the Division of Geological and Planetary Sciences, California Institute of Technology.

[1] T. J. Ahrens, J. Appl. Phys. **43**, 2443 (1972).
[2] J. Kissel and F. R. Krueger, J. Appl. Phys. A **42**, 69 (1987).
[3] S. A. Sandford *et al.*, Science **314**, 1720 (2006).
[4] P. R. Ratcliff and F. Allahdadi, Adv. Space Res. **17**, 1287 (1996).
[5] D. E. Austin, R. L. Grimm, H. L. K. Manning, C. L. Bailey, J. E. Farnsworth, T. J. Ahrens, and J. L. Beauchamp, J. Geophys. Res. Planets **108**, 5038, doi:10.1029/2002JE001947 (2003).
[6] W. K. Hartmann and D. R. Davis, Icarus **24**, 504 (1975).
[7] A. G. W. Cameron and W. R. Ward, in *Lunar and Planetary Science VII* (Lunar Planet. Inst., Houston, 1976), Vol. 120.
[8] E. Belbruno and J. R. Gott III, Astron. J. **129**, 1724 (2005).
[9] G. G. Managadze, W. B. Brinckerhoff, and A. E. Chumikov, Int. J. Impact Engng. **30**, 449 (2003).
[10] G. G. Managadze, JETP J. Exp. Theo. Phys. **97**, 49 (2003).
[11] L. W. Alvarez *et al.*, Science **208**, 109 (1980).
[12] J. D. O'Keefe and T. J. Ahrens, Nature (London) **338**, 247 (1989).
[13] K. O. Pope, K. H. Baines, A. C. Ocampo, and B. A. Ivanov, Earth Planet. Sci. Lett. **128**, 719 (1994).
[14] H. Sigurdsson, S. Dhondt, and S. Carey, Earth Planet. Sci. Lett. **109**, 543 (1992).
[15] R. Brett, Geochim. Cosmochim. Acta **56**, 3603 (1992).
[16] K. Kawaragi, Y. Sekine, T. Kadono, S. Sugita, S. Ohno, K. Ishibashi, K. Kurosawa, T. Matsui, and S. Ikeda, Earth Planet. Sci. Lett. **282**, 56 (2009).
[17] J. B. Pollack, O. B. Toon, T. P. Ackerman, C. P. McKay, and R. P. Turco, Science **219**, 287 (1983).
[18] R. G. Prinn and B. Fegley, Earth Planet. Sci. Lett. **83**, 1 (1987).
[19] P. J. Crutzen, Nature (London) **330**, 108 (1987).
[20] H. J. Melosh, Meteoritics **25**, 386 (1990).
[21] T. J. Ahrens, M. B. Boslough, W. G. Ginn, M. S. Vassiliou, M. A. Lange, J. P. Watt, K. Kondo, R. F. Svendsen, S. M. Rigden, and E. M. Stolper, AIP Conf. Proc. **78**, 631 (1982).
[22] T. N. Tingle, J. A. Tyburczy, T. J. Ahrens, and C. H. Becker, Origins Life Evol. Biosphere **21**, 385 (1992).
[23] J. A. Tyburczy, X. M. Xu, T. J. Ahrens, and S. Epstein, Earth Planet. Sci. Lett. **192**, 23 (2001).
[24] E. M. Mellado, K. Hornung, and J. Kissel, Int. J. Impact Engng. **33**, 419 (2006).

[25]R. Srama, W. Woiwode, F. Postberg, S. P. Ames, S. Fujii, D. Dupin, J. Ormond-Prout, Z. Sternovsky, S. Kempf, G. Moragas-Kiostermeyer, A. Mocker, and E. Grun, Rapid Commun. Mass Spectrom. **23**, 3895 (2009).
[26]J. K. Hillier, S. Sestak, S. F. Green, F. Postberg, R. Srama, and M. Trieloff, Planet. Space Sci. **57**, 2081 (2009).
[27]F. Postberg, M. Trieloff, R. Srama, J. K. Hillier, Z. Gainsforth, A. J. Westphal, S. Bugiel, E. Grun, S. Armes, A. Kearsley, T. Tyliszczak, and W. H. Schwartz, Meteor. Planet. Sci. **45**, A165 (2010).
[28]B. K. Dalmann, E. Grun, J. Kissel, and H. Dietzel, Planet. Space Sci. **25**, 135 (1977).
[29]K. Hornung and J. Kissel, Astron. Astrophys. **291**, 324 (1994).
[30]E. M. Mellado, K. Hornung, R. Srama, J. Kissel, S. P. Armes, and S. Fujii, Int. J. Impact Engng. **38**, 486 (2011).
[31]J. Kissel and R. F. Krueger, Rapid Comm. Mass Spectrom. **15**, 1713 (2001).
[32]J. H. Gross, *Mass Spectrometry* (Springer, 2004), Chap. 2 and 6.